Hybrid Feedback Control Methods
for Robust and Global Power Conversion *

Jun Chai * **Ricardo G. Sanfelice** *

* *University of California, Santa Cruz, CA 95064 USA*
(e-mail: jchai3,ricardo@ucsc.edu).

Abstract: In this paper, the applicability and importance of hybrid system tools for the design of control algorithms for energy conversion in power systems is illustrated in two hybrid control designs, one pertaining to DC/DC conversion and the other to DC/AC inversion. In particular, the mathematical models considered consist of constrained switched differential equations/inclusions that include all possible modes of operation of the systems. Furthermore, the obtained models can be analyzed and their algorithms designed using hybrid system tools so as to attain key desired properties, such as stability, forward invariance, global convergence, and robustness. We argue that hybrid system tools provide a systematic approach for analysis and controller design of power systems. In particular, hybrid system tools usually leads to power quantities that have better performance and robustness to state perturbations. Furthermore, they provide guidelines on how to tune the controller parameters based on design requirements. These factors motivate the implementation of the proposed hybrid controllers in modern power conversion systems that use renewable energy sources. Simulations illustrating the main results and benchmark tests are included.

Keywords: Hybrid systems, Control theory, Power system control, Invariance, Lyapunov Stability

1. INTRODUCTION

Under the name "smart grid," future power generation and distribution systems ought to provide efficient, reliable and environment-friendly power generation, conversion and transmission to customers. In particular, advanced power conversion methods from renewable energy sources are required. Recently developed hybrid system tools have the potential to enable the design of algorithms that address such challenges; see examples in Escobar et al. (1999); Heemels et al. (2003a); Senesky et al. (2003); Geyer et al. (2004); Frasca et al. (2010); Vasca and Iannelli (2012). In this paper, we show that the nonsmooth and recurrent switching mechanisms in power conversion systems demand the use of hybrid system tools for control design of such systems.

We focus on recent designs of hybrid feedback controllers for a DC/DC boost converter and a single-phase DC/AC inverter. The systems involved in these design problems have the following challenging features, which make tools for hybrid systems very fitting (if not mandatory) for their analysis and design:

1) Systems involve nonsmooth dynamics under constraints due to the presence of switches and/or diodes;
2) Stabilization goals require recurrent switching;
3) Systems have state perturbations and unmodeled dynamics.

We show that tools for hybrid systems in Goebel et al. (2012) can be applied to the modeling, controller design, and analysis of these power conversion systems. In particular, key design steps and mathematical analysis in the controller design process for each power converter are outlined. We show that the application of hybrid system theories to power conversion not only provides implementable controllers, but also are useful in highlighting the robustness introduced by such (hybrid) feedback. Simulations for both problems confirm the usefulness of hybrid systems methods in power conversion. In addition, to allow simulation-based quantifiable performance comparison between our control algorithms and others, we propose benchmark tests that focus on switching properties of these power systems. In particular, the proposed benchmark tests are relevant when assessing durability of the switching devices used in hardware/software implementations. Furthermore, we indicate that both control algorithms have the flexibility of changing how often the switches happen by adjusting a corresponding controller parameter.

The remainder of the paper is organized as follows. A short introduction on applying hybrid control theory to power conversion is presented in Section 2. Section 3 highlights the controller designs and analysis using hybrid system tools from Theunisse et al. (2015) and Chai and Sanfelice (2014). Numerical simulations and benchmark test results are also included in Section 3. Finally, concluding remarks are presented in Section 4.

2. THE ROLE OF HYBRID SYSTEMS IN FEEDBACK CONTROL FOR POWER CONVERSION

Most power conversion circuits include some sort of switching mechanism as well as passive components for filtering. The switching mechanisms typically introduce changes in the dynamics, which define different modes of operation and associated discrete dynamics. The passive components for filtering and other analog tasks introduce continuous dynamics into the system. In this way, depending on the configuration of the switches and/or diodes in the circuit, the system operates at different modes and switches between them. By controlling the configuration of the switches with an appropriate algorithm, the closed-loop system generates desired output signals. Popular control algorithms for such purpose are designed using pulse width modulation (PWM), which is a technique that changes the configuration of the switches by comparing a carrier signal (e.g., a triangular signal for DC/AC inverter) and a reference signal (e.g., a sinusoidal signal for DC/AC inverter).
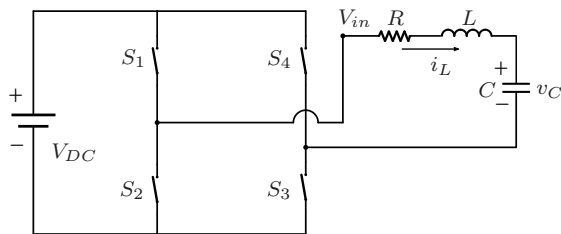
(a) Single-phase DC/AC inverter.
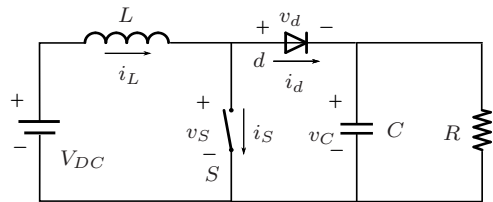
(b) DC/DC boost converter.

Fig. 1. Circuit diagram for two benchmark problems.

Due to the switching nature of these power converters/inverters and the associated continuous dynamics, these systems have nonsmooth dynamics, which can be modeled as differential equations/inclusions with constraints as in Goebel et al. (2012). For example, the single phase DC/AC inverter with H-bridge in Fig. 1a has multiple operation modes, each of them is determined by a different configuration of the switches and leading to a differential inclusion; see Section 3.2.

Unfortunately, the desired output of the systems in Fig. 1 cannot be generated by choosing a single mode of operation for all time. In fact, for each fixed configuration of the switches, the resulting system has an equilibrium point that does not represent the desired output. More precisely, for example, for the circuit in Fig 1a, in which i_L and v_C represent the current though inductor and voltage across the capacitor, when $S_1 = S_3 = \text{ON}$ and $S_2 = S_4 = \text{OFF}$, the resulting equilibrium is for $i_L = 0$ and $v_C = V_{DC}$, while, when $S_1 = S_3 = \text{OFF}$ and $S_2 = S_4 = \text{ON}$, the equilibrium condition is $i_L = 0$ and $v_C = -V_{DC}$ (other equilibrium points can be computed similarly). Due to

this, a control algorithm that changes the configuration of the switches recurrently is required to achieve the desired AC output for the inverter. Similarly, algorithms with the same feature are required for the DC/DC boost converter in Fig. 1b, where the control algorithm needs to switch between two operation modes to generate an approximate DC output signal.

In Theunisse et al. (2015) and Chai and Sanfelice (2014), we model the nonsmooth dynamics of circuits for power conversion, such as those in Fig. 1a, 1b, as well as their algorithms as hybrid systems, for which the framework and tools in Goebel et al. (2012) are employed. In addition to stability properties, the hybrid analysis tools from Goebel et al. (2012) allow us to conclude robustness properties of the power conversion systems. In particular, having the closed-loop systems with designed controller to satisfy conditions in (Goebel et al., 2012, Assumption 6.5) directly leads to robustness to small state perturbations and unmodeled dynamics. Moreover, the same framework also benefits the modeling and analysis of hybrid systems that require periodic-like solutions, which can be studied using the forward invariance of sets; see Section 3.2.

As in Goebel et al. (2012), a hybrid system $\mathcal{H}$ can be written as

$$\mathcal{H} \begin{cases} \dot{z} \in F(z) & z \in \mathcal{C} \\ z^+ \in G(z) & z \in \mathcal{D}, \end{cases} \tag{1}$$

where $\mathcal{C}, F, \mathcal{D}$, and G represent the flow set, the flow map, the jump set, and the jump map, respectively. Solutions to (1) have continuous and/or discrete behavior depending on the system data $(\mathcal{C}, F, \mathcal{D}, G)$. Following Goebel et al. (2012), besides the usual time variable $t \in \mathbb{R}_{\geq 0} := [0, +\infty)$, we consider the number of jumps, $j \in \mathbb{N} := \{0, 1, 2, ...\}$, as an independent variable. Thus, hybrid time is parametrized by (t, j). A solution to the hybrid system (1) is given by a hybrid arc ϕ satisfying the dynamics of (1). For more details about solutions to hybrid systems, see (Goebel et al., 2012, Chapter 2).

Furthermore, the following results from our recent works are important for the purpose of this paper:

- *Hybrid basic conditions* from (Goebel et al., 2012, Assumption 6.5):
(A1) $\mathcal{C}$ and $\mathcal{D}$ are closed subsets of $\mathbb{R}^n$;
(A2) $F : \mathbb{R}^n \rightrightarrows \mathbb{R}^n$ is outer semicontinuous and locally bounded relative to $\mathcal{C}$, $\mathcal{C} \subset \text{dom} F$, and $F(x)$ is convex for every $x \in \mathcal{C}$;
(A3) $G : \mathbb{R}^n \rightrightarrows \mathbb{R}^n$ is outer semicontinuous and locally bounded relative to $\mathcal{D}$, and $\mathcal{D} \subset \text{dom} G$.
- *Forward invariance of a set for hybrid systems* from Chai and Sanfelice (2014):
A set $K \subset \mathbb{R}^n$ is forward invariant for $\mathcal{H}$ if every maximal solution ϕ from K is complete and $\phi(t, j) \in K$ for all $(t, j) \in \text{dom} \phi$.

3. TWO CONTROLLER DESIGN BENCHMARK PROBLEMS IN ENERGY CONVERSION

In this section, we propose the following two controller design benchmark problems in energy conversion:

a) Design a controller for the DC/DC boost converter in Fig. 1b with given system parameters V_{DC}, L, C,

R, such that the closed-loop system outputs a DC-like signal with desired value;

b) Design a controller for the single-phase DC/AC inverter in Fig. 1a with given system parameters V_{DC}, L, C, R, such that the closed-loop system outputs a sinusoidal-like signal with desired amplitude and frequency.

Next, we outline the modeling, stability analysis, and controller designs from our previous works. Complete details of the work in Section 3.1 and Section 3.2 are presented in Theunisse et al. (2015) and Chai and Sanfelice (2014), respectively. Functionality of each proposed controller is proven by presenting both mathematical analysis and numerical simulations. In addition, we propose benchmark tests for each system. For the DC/DC boost converter controller with spatial regulation, we study the number of switches per second during its "steady state;" see Section 3.1. For the DC/AC inverter controller, the benchmark tests consists of determining the number of switches per period of the generated sinusoidal-like signal; see Section 3.2.

3.1 DC/DC Boost Converter

The DC/DC boost converter circuit is shown in Fig. 1b. It consists of a DC voltage source V_{DC}, a capacitor C, an ideal diode d, an inductor L, a resistor R, and an ideal switch S. The voltage across the capacitor is denoted by v_C, and the current through the inductor is denoted by i_L. The presence of switching elements (d and S) causes the overall system to be of switching/hybrid nature. The purpose of the circuit is to draw power from the DC voltage source, and supply power to the load at a higher DC voltage value. This task is accomplished by first closing the switch to store energy in the inductor, and then opening the switch to transfer that energy to the capacitor, where it is available to the load R. Depending on the (discrete) state of an ideal diode and of an ideal switch, one can distinguish four modes of operation, see details in Heemels et al. (2003b) and Theunisse et al. (2015):

> mode 1: $(S = 0, d = 1)$ mode 2: $(S = 1, d = 0)$
> mode 3: $(S = 0, d = 0)$ mode 4: $(S = 1, d = 1)$

where $d = 1$ represents the diode conducting, i.e., $i_d \geq 0, v_d = 0$; $d = 0$ represents the diode blocking current, i.e., $i_d = 0, v_d \leq 0$; $S = 1$ represents when the switch is "ON," i.e., $v_S = 0$; and $S = 0$ represents when the switch is "OFF," i.e., $i_S = 0$. As shown in Theunisse et al. (2015), these four modes can be combined into two modes of operations corresponding to the switch in either "ON" or "OFF" position. Defining $x := (v_C, i_L)$, the dynamics of the DC/DC boost converter can be expressed by two differential inclusions with constraints as follows:

- For each $x \in \widetilde{M_0} := \{x \in \mathbb{R}^2 : i_L \geq 0\}$, we have

$$F_0(x) :=$$
$$\begin{cases} \begin{bmatrix} -\dfrac{1}{RC}v_C + \dfrac{1}{C}i_L \\ -\dfrac{1}{L}v_C + \dfrac{V_{DC}}{L} \end{bmatrix} & \text{if } x \in \{x \in \mathbb{R}^2 : i_L > 0\} \cup \\ & \{x \in \mathbb{R}^2 : i_L = 0, v_C < V_{DC}\} \\ \left\{-\dfrac{1}{RC}v_C\right\} \times \left[-\dfrac{1}{L}v_C + \dfrac{V_{DC}}{L},\ 0\right] \\ & \text{if } x \in \{x \in \mathbb{R}^2 : v_C \geq V_{DC},\ i_L = 0\}. \end{cases}$$

- For each $x \in \widetilde{M_1} = \{x \in \mathbb{R}^2 : v_C \geq 0\}$, we have

$$F_1(x) := \begin{bmatrix} -\dfrac{1}{RC}v_C & \dfrac{V_{DC}}{L} \end{bmatrix}^\top.$$

We introduce a switching variable $q \in \{0, 1\}$ to model the selection made by the control algorithm. Since q would be constant in between switches, the flow map of the resulting system as in (1) would be

$$F(x, q) = \begin{bmatrix} F_q(x) \\ 0 \end{bmatrix} \qquad \text{for each } q \in \{0, 1\}.$$

Notice that the switching variable q can be either 0 or 1, representing different (set-valued) vector fields, which, at every instant, depends on the choice made by the controller. This promotes the use of hybrid system analysis and controller design tools.

As stated in benchmark problem a), the goal of the controller is to approximate a DC output with given v_C^* and i_L^*,[1] which represent the desired voltage cross capacitor and current through inductor, respectively. The equivalent design goal is to design a controller that guarantees asymptotic stability of set $\mathcal{A}_x \times \{0, 1\}$ for the closed-loop system, where $\mathcal{A}_x := \{x \in \mathbb{R}^2 : x = x^*\}$ and $x^* = (v_C^*, i_L^*)$.

The hybrid controller proposed to achieve the desired DC voltage output is based on the following control Lyapunov function:

$$V(x) = (x - x^*)^\top P (x - x^*), \text{ where } P = \begin{bmatrix} p_{11} & 0 \\ 0 & p_{22} \end{bmatrix}.$$

For each $q \in \{0, 1\}$, let $\gamma_q(x) := \max_{\xi \in F_q(x)} \langle \nabla V(x), \xi \rangle$, and $\widetilde{\gamma}_q(x)$ be given for each $x \in \mathbb{R}^2$ as

$$\widetilde{\gamma}_0(x) = \gamma_0(x) + K_0 (v_C - v_C^*)^2$$
$$\widetilde{\gamma}_1(x) = \gamma_1(x) + K_1 (v_C - v_C^*)^2,$$

where $K_0 \in \left(0, \frac{2p_{11}}{RC}\right)$, $K_1 \in \left(0, \frac{2p_{11}}{RC}\right)$. Then, the control law is designed such that we have $\widetilde{\gamma}_q(x) \leq 0$ for each $x \in \mathbb{R}^2, q \in \{0, 1\}$. The closed-loop system with this proposed controller can be expressed as in (1) with state variable $z = [x\ q]^\top$ and dynamics

$$\dot{z} \in \begin{bmatrix} F_q(x) \\ 0 \end{bmatrix} =: F(z) \qquad z \in \mathcal{C}$$
$$z^+ = \begin{bmatrix} x \\ 1 - q \end{bmatrix} =: G(z) \qquad z \in \mathcal{D} \tag{2}$$

where $\mathcal{C} = \{z \in \mathbb{R}^2 \times \{0, 1\} : x \in \widetilde{M_q}, \widetilde{\gamma}_q(x) \leq 0, q \in \{0, 1\}\}$ and $\mathcal{D} = \{z \in \mathbb{R}^2 \times \{0, 1\} : x \in \widetilde{M_q}, \widetilde{\gamma}_q(x) = 0, q \in \{0, 1\}\}$.

Assuming all system parameters are positive, $\frac{p_{11}}{C} = \frac{p_{22}}{L}$, $v_C^* > V_{DC}$, and $i_L^* = \frac{v_C^{*2}}{RV_{DC}}$, it can be shown that the set $\mathcal{A}_x \times \{0, 1\}$ is globally asymptotic stable for the closed-loop system; see (Theunisse et al., 2015, Theorem IV.5). In addition, a design result is established in (Theunisse et al., 2015, Lemma III.3), which permits tuning the switching "frequency" between system modes by properly choosing constants K_0 and K_1.

Simulation results for the closed-loop system $\mathcal{H}$, shown in Fig. 2, used the following system parameters:[2]

---

[1] In fact, i_L^* is a function of v_C^* for given system parameters V_{DC}, L, R, C.

[2] All simulations of the closed-loop system $\mathcal{H}$ are performed using the Hybrid Equations (HyEQ) Toolbox (see Sanfelice et al. (2013)).

$V_{DC} = 5V$, $R = 3\Omega$, $C = 0.1F$, $L = 0.2H$, $P = \begin{bmatrix} C/2 & 0 \\ 0 & L/2 \end{bmatrix}$, and $x^* = (7, 3.27)$. As can be seen, the solution components (v_C, i_L) of the closed-loop system converge from the given initial condition to the globally asymptotic stable set $\mathcal{A}_x$.
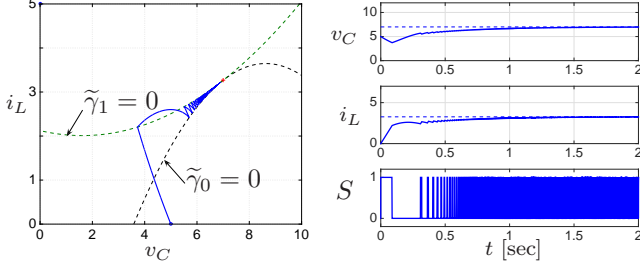

Fig. 2. Simulation results for the closed-loop system $\mathcal{H}$ with initial conditions $x_0 = (5, 0)$, $q_0 = 0$, using $K_0 = 0.05$, $K_1 = 0.12$.

In addition, the construction of the proposed controller is such that the closed-loop system $\mathcal{H}$ has data satisfying the hybrid basic conditions (A1)-(A3). With these properties, we have that the asymptotic stability property is robust to small perturbations, such as state noise and unmodeled system dynamics; see (Theunisse et al., 2015, Theorem IV.6).

Furthermore, the fact that (A1)-(A3) are satisfied implies that the closed-loop system is robust to spatial regularization. More precisely, we use the condition $\widetilde{\gamma}_q(x) = \rho$ rather than $\widetilde{\gamma}_q(x) = 0$ as switching boundaries at the controller level, where ρ is a small positive constant. The motivation for such a modification is to reduce the number of switches and enlarge the time between switches by allowing a neighborhood around x^* between the two switching boundaries, rather than having them intersect at the point x^*. The regularized system is denoted as [3]

$$\mathcal{H}_\rho = (\mathcal{C}_\rho, F, \mathcal{D}_\rho, G). \qquad (3)$$

Under the given assumptions, it can be shown that the closed-loop solutions satisfy a practical $\mathcal{KL}$ bound from compact sets, namely, for every $\epsilon > 0$ and compact set $K \subset \mathbb{R}^2$, it is such that the solutions to the closed-loop system from $K \times \{0, 1\}$ converge to a neighborhood of $\mathcal{A}_x \times \{0, 1\}$ after finite hybrid time (which depends on ϵ). For more details, see (Theunisse et al., 2015, Theorem IV.7).

Using the regularized system in (3), we propose the following benchmark test for the DC/DC boost converter: given a constant ϵ representing the maximum deviation of the output range v_C from v_C^*, determine the average number of switches per second after the solutions reach the set $\{z \in \mathbb{R}^2 \times \{0, 1\} : |v_C - v_C^*| \le \epsilon\}$ and remain in it. Moreover, we also compute the average number of switches and its standard deviation (Std) as a function of ϵ. We use the same system parameters and the relationship $\epsilon \approx 1.3\rho$ from (Theunisse et al., 2015, Table II) for this benchmark test. In addition, for each value of ϵ, we present the average

---

[3] See (Theunisse et al., 2015, Section IV.E) for details on definitions of system data.

dwell time for switching. The number of switches per second reported are rounded.

Table 1. Benchmark test for DC/DC boost converter.

ϵ	x_0	Average number of switches per second	Average & Std	Average dwell-time between switches
0.01	(0,5)	1467	Average = 1587 Std = 61.21	S = ON : $9 \times 10^{-4}s$ S = OFF : $3.6 \times 10^{-4}s$
	(4,3)	1625		
	(6,2)	1625		
	(3,8)	1592		
	(5,0)	1625		
0.05	(0,5)	348	Average = 356 Std = 4.37	S = ON : $4 \times 10^{-3}s$ S = OFF : $1.6 \times 10^{-3}s$
	(4,3)	360		
	(6,2)	360		
	(3,8)	355		
	(5,0)	359		
0.1	(0,5)	179	Average = 179 Std = 0.075	S = ON : $8 \times 10^{-3}s$ S = OFF : $3.1 \times 10^{-3}s$
	(4,3)	179		
	(6,2)	179		
	(3,8)	179		
	(5,0)	179		

The numerical results in Table 1 indicate that, for smaller values of ϵ, switching happens more frequently. While the number of switches varies slightly with the initial condition, the standard deviations suggest that the dispersion around the average is small. In addition, the average dwell time results indicate that the switch stays at the "ON" position longer than at the "OFF" position, which is expected, but more importantly, indicate that the time between consecutive switching times has a reasonable lower bound. Such lower bound gives an indication of how fast the switch happens during the "steady state."

3.2 Single-Phase DC/AC Inverter

A single-phase DC/AC inverter circuit consists of four controlled switches connecting to a series RLC filter, as shown in Fig. 1a. The DC signal V_{DC} is the input to the inverter. The output signal v_C denotes the voltage across the capacitor C, and i_L denotes the current through the inductor L. The objective of a controller selecting the positions of the switches $S_1 - S_4$ is to generate an output v_C that approximates a sinusoidal signal by appropriately toggling the switches. The presence of switches in the circuit introduces nonsmooth dynamics. By controlling the position of the switches, to either "ON" or "OFF" position, the voltage V_{in} to the RLC filter will equal either V_{DC}, $-V_{DC}$, or 0. The dynamics of the system are

$$\begin{bmatrix} \dot{i}_L \\ \dot{v}_C \end{bmatrix} = f_q(x) := \begin{bmatrix} \dfrac{V_{DC}}{L}q - \dfrac{R}{L}i_L - \dfrac{1}{L}v_C \\ \dfrac{1}{C}i_L \end{bmatrix}, \qquad (4)$$

where R, L, C are parameters of the circuit, $x := (i_L, v_C) \in \mathbb{R}^2$, and $q \in Q := \{-1, 0, 1\}$ is a logic variable that describes the position of the switches. We have $q = 1$ when $S_1 = S_3 = $ ON and $S_2 = S_4 = $ OFF; we have $q = -1$, when $S_1 = S_3 = $ OFF and $S_2 = S_4 = $ ON; and we have $q = 0$ when $S_1 = S_4 = $ OFF and $S_2 = S_3 = $ ON. Notice that each value of the switching variable q represents a different vector field, which, at every instant, depends on the choice made by the controller. This promotes the use of hybrid system analysis and controller design tools.

As stated in benchmark problem b), the controller design goal is to generate a sinusoidal-like voltage output across

the capacitor C. In particular, the desired signal is a steady state (oscillatory) response of the RLC filter in Fig. 1a to a sinusoidal input signal $t \mapsto V_{in}(t) = A\sin(\omega t + \theta)$, where $A, \omega > 0$ are the amplitude and angular frequency, respectively, and θ is the initial phase. Using the equations of the filter, under the effect of the input $t \mapsto V_{in}(t)$, every steady state solution, in particular, (i_L^*, v_C^*), satisfies $V(i_L^*(t), v_C^*(t)) = c$ for all $t \geq 0$ and some positive constant c, where

$$V(x) := \left(\frac{i_L}{a}\right)^2 + \left(\frac{v_C}{b}\right)^2 \quad x \in \mathbb{R}^2 \tag{5}$$

with constants $a := \frac{1}{\sqrt{R^2 + (L\omega - \frac{1}{C\omega})^2}}$, and $b := \frac{a}{C\omega}$.

A hybrid control strategy is developed for the inverter to switch among the three operation modes described previously, which guarantees that the output trajectory converges to a region (tracking band) that is defined as a neighborhood around the set $\{x \in \mathbb{R}^2 : V(x) = c\}$. More precisely, given c_i and c_o such that $c_i < c < c_o$, the tracking band is given by $\{x \in \mathbb{R}^2 : c_i \leq V(x) \leq c_o\}$. On the (i_L, v_C) plane, the tracking band has an outer boundary given by $S_o = \{x \in \mathbb{R}^2 : V(x) = c_o\}$, and an inner boundary given by $S_i = \{x \in \mathbb{R}^2 : V(x) = c_i\}$. The reference trajectory, is enclosed by the tracking band. A trajectory to (4) with the proposed control strategy ought to remain in the tracking band for all time while describing a periodic-like orbit.

The feedback control architecture for such a hybrid controller is shown in Fig. 3, where $p \in P := \{1, 2\}$ is a logic variable that select between controller $\mathcal{H}_{fw}$ and $\mathcal{H}_g$; see Chai and Sanfelice (2014) for detailed definitions and analysis of the three controllers $\mathcal{H}_s$, $\mathcal{H}_{fw}$ and $\mathcal{H}_g$.
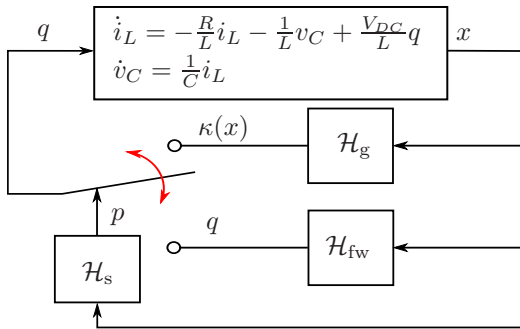

Fig. 3. Full closed-loop system with $\mathcal{H}_s, \mathcal{H}_g$, and $\mathcal{H}_{fw}$. (Chai and Sanfelice, 2014, Fig. 4)

A key result, see (Chai and Sanfelice, 2014, Proposition 1), for the closed-loop system with $\mathcal{H}_{fw}$ in the loop, i.e., $\mathcal{H}_{fw}^{cl} = (\mathcal{C}_{fw}, f_{fw}^{cl}, \mathcal{D}_{fw}, G_{fw}^{cl})$, is the *forward invariance* of the set $\mathcal{T} := Q \times \{x \in \mathbb{R}^2 : V(x) \in [c_1, c_o]\}$ for $\mathcal{H}_{fw}^{cl}$. This property is guaranteed by the inner product properties of (4) and the Lyapunov-like function V in (5); see (Chai and Sanfelice, 2014, Lemma 2). Furthermore, the closed-loop system data $(\mathcal{C}_{fw}, f_{fw}^{cl}, \mathcal{D}_{fw}, G_{fw}^{cl})$ satisfies conditions (A1)-(A3); see (Chai and Sanfelice, 2014, Lemma 1). Thus, according to (Goebel et al., 2012, Section 6.1), the behavior of the hybrid closed-loop system $\mathcal{H}_{fw}^{cl}$ is robust to small perturbations.

As a result, the full closed-loop system that combines the dynamics of the three controllers, $\mathcal{H}_{fw}$, $\mathcal{H}_g$ and $\mathcal{H}_s$, is autonomous and has state variable $z = (p, q, x)$ (with some abuse of notations). Its hybrid model is given as in (1), where the flow map f is given as

$$f(z) = \begin{bmatrix} 0 \\ 0 \\ -\frac{R}{L}i_L - \frac{1}{L}v_C + \frac{V_{DC}}{L}q \\ \frac{1}{C}i_L \end{bmatrix},$$

the flow set $\mathcal{C}$ is given as

$\mathcal{C} = \{z \in \mathcal{Z} : p = 1, (q, x) \in \mathcal{C}_{fw}\} \cup \{z \in \mathcal{Z} : p = 2, x \in \mathcal{C}_g\}$,

where $\mathcal{Z} := P \times Q \times \mathbb{R}^2$, the jump map is given as

$$G(z) = \begin{bmatrix} 1 \\ G_{fw}(q) \\ i_L \\ v_C \end{bmatrix},$$

and the jump set is given as

$\mathcal{D} = \{z \in \mathcal{Z} : (p, x) \in \mathcal{D}_s\} \cup \{z \in \mathcal{Z} : p = 1, (q, x) \in \mathcal{D}_{fw}\}$
$\cup \{z \in \mathcal{Z} : p = 2, x \in \mathcal{D}_g\}$.

With further analysis, it can be shown that the set $\mathcal{T}$ is globally asymptotically stable for the full closed-loop system; see (Chai and Sanfelice, 2014, Theorem 1).

Next, we show a simulation confirming that the proposed controller is robust to variations of V_{DC}, which is a key robustness property of our controller. The following system constants are used: $R = 0.7\Omega$, $L = 0.106H$, $C = 0.663\mu F$, $\omega = 120\pi$ (or, equivalently, the frequency is 60 Hz), $\epsilon = 0.042$, $c_o = 1.1$, $c_i = 0.9$, $b = 120\sqrt{2}$, and $c = 1$. The initial condition $x(0, 0) = (3\sqrt{2}, 0)$ is used in this simulation.
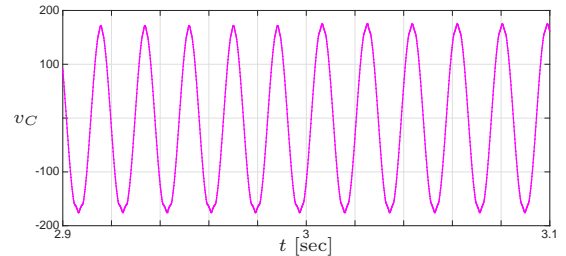
(a) v_C output of the single-phase inverter controlled by our hybrid algorithm with a step change in V_{DC} at 3s.
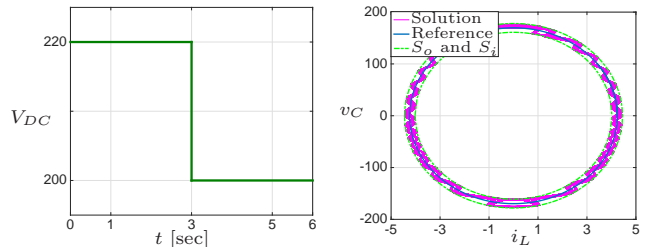
(b) Step V_{DC} signal at 3s.

(c) Corresponding trajectory on $\mathbb{R}^2$ of inverter with hybrid controller.

Fig. 4. Simulations with a step in V_{DC} at 3s.

Fig. 4a shows the output voltage v_C close to its steady state that is preserved even after a step change in V_{DC}

from $220V$ to $200V$ at $3s$ (see Figure 4b). A Fast Fourier Transform (FFT) analysis is also performed to show that the output signal has the desired frequency; see (Chai and Sanfelice, 2014, Fig. 6a).

In addition to the functionality of the proposed controller, one can tune the width of the "tracking band" to assure that the output trajectory is close as desired to the ideal trajectory on the $\mathbb{R}^2$ plane. However, the thinner the tracking band, the larger the number of switches within a "period" are. Thus, we propose a benchmark test for control algorithms of single-phase DC/AC inverters that focuses on the switching properties of the designed controllers. More precisely, we are interested in the average number of switches during one "period" of the output sinusoidal-like signal v_C of the closed-loop system. In this benchmark test, for different value of c_i and c_o, we record the average number of switches during a time period of $\frac{2\pi}{\omega}$ after the "transient" state of solutions from five different initial conditions.[4] In addition, we also compute the average number of switches and its standard deviation (Std) for three different widths $c_o - c_i$ of the tracking band. The numbers of switches per period are rounded.

Table 2. Benchmark test for single-phase DC/AC inverter.

c_i & c_o	x_0	Average number of switches per period	Average & Std
$c_i = 0.9$ $c_o = 1.1$ $c_o - c_i = 0.2$	$(3\sqrt{2},0)$	3277	Average = 3230 Std = 105
	$(1.06, 164.32)$	3123	
	$(2.12, 146.97)$	3348	
	$(3.18,112.25)$	3114	
	$(0, 120\sqrt{2})$	3289	
$c_i = 0.95$ $c_o = 1.05$ $c_o - c_i = 0.1$	$(3\sqrt{2},0)$	6557	Average = 6432 Std = 231
	$(1.06, 164.32)$	6397	
	$(2.12, 146.97)$	6604	
	$(3.18,112.25)$	6042	
	$(0, 120\sqrt{2})$	6559	
$c_i = 0.99$ $c_o = 1.01$ $c_o - c_i = 0.02$	$(3\sqrt{2},0)$	3.18e4	Average = 3.18e4 Std = 219
	$(1.06, 164.32)$	3.14e4	
	$(2.12, 146.97)$	3.19e4	
	$(3.18,112.25)$	3.17e4	
	$(0, 120\sqrt{2})$	3.19e4	

Table 2 shows that with smaller width of the tracking band (namely, higher precision), switching is more frequent, which is expected. Furthermore, the number of switches varies with different initial conditions, but the average and standard deviation results reported in Table 2 imply that by tuning the value of c_o and c_i, it is possible to control the number of switches per "period." The resulting data also gives a general guideline for choosing appropriate c_o and c_i values for given system parameters.

4. CONCLUSION

The switching nature of power conversion systems requires modeling and analysis tools that can handle both discrete and continuous dynamics, which promote the use of hybrid system tools for modeling, analysis, and controller design. To illustrate such a methodology, two control design benchmark problems, one for a DC/DC boost converter and the other for a single-phase DC/AC inverter, are solved taking a hybrid control systems approach. Benchmark tests characterizing the switching properties of the closed-loop systems are also proposed. The benchmark test results obtained for the proposed algorithms can be used as baseline results to compare with other algorithms in the literature, such as PWM-based controllers.

Additional benchmark tests involving analysis of transient response of closed-loop systems can be developed. In particular, for the DC/DC boost converter, one can characterize the time it takes and the number of switches needed to reach a neighborhood of the desired steady state value of the output. Also, for the single-phase DC/AC inverter, one could be interested in computing the time it takes and the number of switches needed for the output voltage v_C to be desired sinusoidal. Another potential benchmark test could focus on comparing the energy efficiency of the control algorithms.

REFERENCES

Chai, J. and Sanfelice, R.G. (2014). A robust hybrid control algorithm for a single-phase DC/AC inverter with variable input voltage. In *American Control Conference (ACC), 2014*, 1420–1425. IEEE.

Escobar, G., Van Der Schaft, A.J., and Ortega, R. (1999). A hamiltonian viewpoint in the modeling of switching power converters. *Automatica*, 35(3), 445–452.

Frasca, R., Camlibel, M.K., Goknar, I., Iannelli, L., and Vasca, F. (2010). Linear passive networks with ideal switches: Consistent initial conditions and state discontinuities. *IEEE Transactions on Circuits and Systems I: Regular Papers*, 57(12), 3138–3151.

Geyer, T., Papafotiou, G., and Morari, M. (2004). On the optimal control of switch-mode DC/DC converters. In *Hybrid systems: Computation and control*, 342–356. Springer.

Goebel, R., Sanfelice, R.G., and Teel, A.R. (2012). *Hybrid Dynamical Systems: Modeling, Stability, and Robustness.* Princeton University Press, New Jersey.

Heemels, W., Çamlıbel, M.K., Van Der Schaft, A., and Schumacher, J. (2003a). Modelling, well-posedness, and stability of switched electrical networks. In *Hybrid Systems: Computation and Control*, 249–266. Springer.

Heemels, W., Camlibel, M., Schaft, A., and Schumacher, J. (2003b). Modelling, well-posedness, and stability of switched electrical networks. In O. Maler and A. Pnueli (eds.), *Hybrid Systems: Computation and Control*, volume 2623 of *Lecture Notes in Computer Science*, 249–266. Springer Berlin Heidelberg.

Sanfelice, R.G., Copp, D.A., and Nanez, P. (2013). A toolbox for simulation of hybrid systems in Matlab/Simulink: Hybrid Equations (HyEQ) Toolbox. In *Proceedings of Hybrid Systems: Computation and Control Conference*, 101–106.

Senesky, M., Eirea, G., and Koo, T.J. (2003). Hybrid modelling and control of power electronics. In *Hybrid Systems: Computation and Control*, 450–465. Springer.

Theunisse, T., Chai, J., Sanfelice, R.G., and Heemels, W.M. (2015). Robust global stabilization of the DC/DC boost converter via hybrid control. *IEEE Transactions on Circuits and Systems I: Regular Papers*, 62(4), 1052–1061.

Vasca, F. and Iannelli, L. (2012). *Dynamics and Control of Switched Electronic Systems.* Springer.

---

[4] By "transient" we mean the time before trajectories enter the set $\mathcal{T}$.